

## Short communication

# The role of biomass burning agricultural emissions in the Indo-Gangetic Plains on the air quality in New Delhi, India

Casey D. Bray\*, William H. Battye, Viney P. Aneja

Department of Marine, Earth and Atmospheric Sciences, North Carolina State University, Raleigh, NC, USA



## ARTICLE INFO

## Keywords:

Agricultural burning emissions  
Indo-gangetic plains  
New Delhi PM<sub>2.5</sub>

## ABSTRACT

Agricultural residue burning in the Indo-Gangetic Plains (IGP) releases large amounts of reactive nitrogen, among other pollutants, into the atmosphere each year. This study focuses on rice paddy residue burning and wheat residue burning during October–November and April–May, respectively, in 2016 and 2017. Emissions of reactive nitrogen species (ammonia (NH<sub>3</sub>), nitrous oxide (N<sub>2</sub>O) and oxides of nitrogen (NO<sub>x</sub> = NO + NO<sub>2</sub>)) were estimated for the study period using a suite of satellite products from the Moderate Resolution Imaging Spectroradiometer (MODIS) sensor on the National Aeronautics and Space Administration (NASA) Aqua and Terra satellites. Emissions were compared against ambient concentrations of fine particulate matter (PM<sub>2.5</sub>) in New Delhi, India, to help determine the impact that these agricultural burns have on PM<sub>2.5</sub>, which is known to have numerous health and environmental impacts associated with prolonged exposure to elevated concentrations. Daily average measured concentrations of PM<sub>2.5</sub> in New Delhi range from 22.43 μg m<sup>-3</sup> to 718.94 μg m<sup>-3</sup> (average 127.15 μg m<sup>-3</sup> ± 95.23 μg m<sup>-3</sup>), with the daily average PM<sub>2.5</sub> concentration exceeding the national ambient air quality standard of 60 μg m<sup>-3</sup> approximately 75% of the time. Concentrations of PM<sub>2.5</sub> were found to peak during October–November, which corresponds with rice paddy residue burning in the IGP. In addition to this, statistical regression models were created to predict average daily PM<sub>2.5</sub> concentrations in New Delhi, India, based on emissions of NH<sub>3</sub> and organic carbon (OC) in the IGP as well as meteorological conditions. The regression model predicted ambient PM<sub>2.5</sub> concentrations ranging from 35 to 719 μg m<sup>-3</sup>. The average modeled concentrations of PM<sub>2.5</sub> in New Delhi, India, were 111 μg m<sup>-3</sup> (standard deviation: ± 23 μg m<sup>-3</sup>) during April/May and 207 ± 87 μg m<sup>-3</sup> during October/November. Both regression models (for wheat residue burning and for rice paddy residue burning) were comparable to the average observations (normalized mean bias less than 0.1%).

## 1. Introduction

Biomass burning (wildfires, prescribed burns and agricultural burns) are known to emit large amounts of pollutants into the atmosphere and contribute to poor air quality at both the local and regional scale (Scholes et al., 1996; Andreae and Merlet, 2001; Freitas et al., 2005; Arola et al., 2007). Each year, extensive agricultural burning occurs in the Indo-Gangetic Plains (IGP; primarily in Punjab, Haryana, and western Uttar Pradesh), which is known as the ‘bread basket’ of India because it produces nearly 2/3 of India's food grains (wheat-rice crop rotation) (Sharma et al., 2011; Kaskaoutis et al., 2014). The rice paddy residue is burned in October–November, while the remaining wheat residue is burned in April–May (Vadrevu et al., 2011; Singh and Kaskaoutis, 2017). The burning of agricultural residue emits particulate matter and trace gasses into the atmosphere, including methane (CH<sub>4</sub>),

carbon monoxide (CO), reactive nitrogen species (Nr; e.g. NH<sub>3</sub>, NO<sub>x</sub>, N<sub>2</sub>O), sulfur dioxide (SO<sub>2</sub>), and hydrocarbons (Gupta et al., 2004). These trace gases can also contribute to the formation of secondary fine particulate matter (PM<sub>2.5</sub>) both at a local and regional scale. In addition to emissions of smoke, high humidity and lower temperatures contribute to severe fog conditions in India during the winter months (Kharol et al., 2012). This fog and smoke contribute to extremely poor air quality that impacts close to 900 million people, which is roughly 1/8th of the world's population (Singh and Kaskaoutis, 2017). In urban areas, such as New Delhi, emissions from agricultural burning in the IGP region are mixed with other anthropogenic emission sources (e.g. power plants, mobile exhaust, ect.) and dust, which elevates concentrations of PM<sub>2.5</sub> to dangerous levels (Bisht et al., 2015; Pant et al., 2015; Shyamsundar et al., 2019). Exposure to these elevated concentrations of fine particulate matter is associated with a number of

\* Corresponding author.

E-mail address: [cdbray@ncsu.edu](mailto:cdbray@ncsu.edu) (C.D. Bray).<https://doi.org/10.1016/j.atmosenv.2019.116983>

Received 10 April 2019; Received in revised form 10 September 2019; Accepted 15 September 2019

Available online 19 September 2019

1352-2310/ © 2019 Elsevier Ltd. All rights reserved.

adverse health effects, such as chronic bronchitis, aggravated asthma, irregular heartbeat, other cardiovascular and respiratory issues and even death (Pope et al., 2002, 2009; Schwartz et al., 2002; Pope and Dockery, 2006; Crouse et al., 2015). PM<sub>2.5</sub> is also associated with several environmental impacts, such as reducing visibility and changing the earth's radiational balance (Fan et al., 2005; Behera and Sharma, 2010; Heald et al., 2012; Wang et al., 2012; Batty et al., 2017). The objectives of this study are to quantify emissions from agricultural burning of both rice paddy residue (October–November) and wheat residue (April–May) in the IGP for 2016–2017 and determine the impact that the agricultural biomass burning emissions have on PM<sub>2.5</sub> concentrations in New Delhi, India. Furthermore, a statistical regression analysis was performed which projects concentrations of PM<sub>2.5</sub> in New Delhi, based on emissions of NH<sub>3</sub> and organic carbon (OC) from agricultural burning in the IGP plains. NH<sub>3</sub> reacts with other air pollutants in the atmosphere to create PM<sub>2.5</sub> in a complex nonlinear relationship between NH<sub>3</sub> emissions and PM<sub>2.5</sub> (Baek and Aneja, 2004; Baek et al., 2004; Paulot and Jacob, 2014). Organic carbon can be used as a surrogate for biomass burning (Ni et al., 2017).

## 2. Data and methodology

Emissions of reactive nitrogen species from agricultural burning in the IGP were calculated based on the following equation (Equation (1), Seiler and Crutzen, 1980):

$$E_i = BA \times B \times FB \times EF_i \quad (1)$$

where  $E_i$  is the emission of species  $i$  (in this case, OC, NH<sub>3</sub>, N<sub>2</sub>O and NO<sub>x</sub>; in g), BA is the area burned (m<sup>2</sup>), B is the biomass loading (kg m<sup>-2</sup>), FB is the fraction of biomass burned in the fire and  $EF_i$  is the emission factor (g kg Biomass Burned<sup>-1</sup>) of species  $i$ . The Moderate Resolution Imaging Spectroradiometer (MODIS) Burned Area product (MCD64A1, Collection 6) was used to determine the area burned (Giglio et al., 2015). This product maps global burned area at a 500 m spatial resolution. Compared to its predecessor (MCD45, Roy et al., 2002; Roy et al., 2005; Roy et al., 2008; Giglio et al., 2018), this product maps 26% more burned area globally and shows reduced uncertainty when compared against the MODIS active fire product (Giglio et al., 2018). The biomass loading (B) values used in this study were 0.593 kg/m<sup>2</sup> for wheat residue burning in April–May and 1.18 kg/m<sup>2</sup> for rice paddy residue burning in October–November, based on literature values from Rajput et al. (2014). To determine the land cover type, the MODIS Global Cropland Extent product was used (Pittman et al., 2010). This product maps the global cropland extent at a 250 m spatial resolution. To determine the fraction of biomass burned, the methodology of Ito and Penner (2004) and Wiedinmyer et al. (2006, 2011) coupled with the MODIS Vegetation Continuous Fields product (MOD44B, Collection 6) were used, which gives the total percent of vegetation at a 250 m spatial resolution (Dimiceli et al., 2015; DiMiceli et al., 2017). The emission factors used in this study are represented in Table 1. For this work, it is assumed that the agricultural burns in the

**Table 1**

Emission factors for reactive nitrogen species used in this work. (source: Ravindra et al., 2019).

	Rice Paddy Residue (g kg <sup>-1</sup> )	Wheat Residue (g kg <sup>-1</sup> )
NH <sub>3</sub>	4.10 <sup>a</sup>	1.30 <sup>c</sup>
NO <sub>x</sub>	2.28 <sup>a</sup>	1.70 <sup>b</sup>
N <sub>2</sub> O	0.48 <sup>b</sup>	0.74 <sup>b</sup>
OC	7.6 <sup>d</sup>	1.2 <sup>d</sup>

<sup>a</sup> Kanabkaew and Oanh (2011).

<sup>b</sup> Sahai et al., 2011

<sup>c</sup> Yang et al., 2008.

<sup>d</sup> Rajput et al. (2014) (adapted from Kanokkanjana et al., 2011 for rice paddy residue burning and Hays et al., 2005 for wheat residue burning).

**Table 2**

Uncertainties in each parameter used to calculate emissions for each pollutant. The combined uncertainty represents the average uncertainty for each fire in New Delhi during the periods of interest.

	Uncertainty April–May	Uncertainty October–November
Burn Area (m <sup>2</sup> )	32,916 <sup>a</sup>	30,055 <sup>a</sup>
Fraction of Biomass Burned	0.013 <sup>a</sup>	0.426 <sup>a</sup>
Biomass Loading (kg m <sup>-2</sup> )	0.178 <sup>b</sup>	0.294 <sup>b</sup>
Emission Factor (g kg Biomass Burned <sup>-1</sup> )		
NH <sub>3</sub>	0.75 <sup>c</sup>	1.24 <sup>d</sup>
NO <sub>x</sub>	1.68 <sup>e</sup>	0.59 <sup>f</sup>
N <sub>2</sub> O	0.46 <sup>e</sup>	0.45 <sup>e</sup>
OC	0.03 <sup>g</sup>	1.2 <sup>g</sup>
Combined Uncertainty (g)		
NH <sub>3</sub>	57.13 <sup>h</sup>	4667.62 <sup>h</sup>
NO <sub>x</sub>	127.96 <sup>h</sup>	2220.88 <sup>h</sup>
N <sub>2</sub> O	35.04 <sup>h</sup>	1693.89 <sup>h</sup>
OC	2.29 <sup>h</sup>	4517.05 <sup>h</sup>

<sup>a</sup> Standard deviation, calculated from this work.

<sup>b</sup> Adapted from Badarinath et al. (2006), following the work of Sahai et al. (2011).

<sup>c</sup> Adapted from Yang et al. (2008), following work of Sahai et al. (2011).

<sup>d</sup> Christian et al. (2003) via Sahai et al. (2011)

<sup>e</sup> Kanabkaew and Oanh (2011) via Ravindra et al. (2019).

<sup>f</sup> Adapted from Kanabkaew and Oanh (2011), following the work of Sahai et al. (2011).

<sup>g</sup> Kanokkanjana et al. (2011) for rice paddy residue burning and Hays et al. (2005) for wheat residue burning via Rajput et al. (2014).

<sup>h</sup> Calculated following the methodology of Sahai et al. (2011).

IGP during April–May are primarily wheat residue and that the agricultural burns for October–November are primarily rice paddy residue (Vadrevu et al., 2011). It is important to note that there is a significant amount of uncertainty associated with each of the satellite products used in this work, and thus also with the emission estimates derived in this work. The uncertainties represented for each product and the combined uncertainties for emissions are given in Table 2. The methodology used to calculate the uncertainties in this work were derived following the work of Sahai et al. (2011), which was adapted from the Eurachem guide (Eurachem/CITAC Working Group, 2000).

The PM<sub>2.5</sub> ambient data were obtained from the OpenAQ Platform (openaq.org) and originate from data.gov.in (an open government data platform) and Central Pollution Control Board (CPCB) (https://app.cpcbccr.com). The meteorological data used in this study were obtained using Modern-Era Retrospective analysis for Research and Applications, Version 2 (Global Modeling and Assimilation Office (GMAO), 2015) datasets: M2I1NXLFO (surface) and M2T1NXSLV (850 m). MERRA-2 data are derived from both observational data and modeled fields into a 0.5° x 0.625° spatial resolution gridded meteorological dataset (Rienecker et al., 2011). For more information on the MERRA and MERRA-2 datasets, refer to Rienecker et al. (2011) and Gelaro et al. (2017). These data can be obtained from the NASA GES DISC website (https://disc.gsfc.nasa.gov/). Finally, active fire data were obtained from NASA's Fire Information for Research Management system (FIRMS) MODIS Active Fire Products (MCD14DL, Collection 6). The active fire product represents the center of a 1 km pixel that contains one or more fires within the pixel based on the MODIS MOD14/MYD14 Fire and Thermal Anomalies algorithm (Giglio et al., 2003).

Regression models that account for both emissions of reactive nitrogen species from agricultural burning and meteorological conditions were created to predict PM<sub>2.5</sub> concentrations in New Delhi, India, using SASv9.4. The regressions were created using the stepwise function, which tests a variety of combination of variables (e.g. the first step will be the best one variable model, the second step will be the best two variable model, etc.). The regression equation chosen for this work was the best fit regression with the highest R<sup>2</sup>. Those variables that are not

selected in the regression are deemed insignificant by SAS (i.e. the variables did not meet the 0.15 significance level). The created regressions predict  $PM_{2.5}$  in New Delhi, India, as a function  $NH_3$  and OC emissions from agriculture residue burning in the IGP and meteorological conditions in New Delhi.  $NH_3$  is an important precursor gas for inorganic  $PM_{2.5}$  constituents, which account for approximately ~28% of  $PM_{2.5}$  concentrations in New Delhi (Sharma and Mandal, 2017). OC accounts for approximately 50% of emissions from agricultural burning (Rajput et al., 2016) and approximately 15% of  $PM_{2.5}$  concentrations in New Delhi (Sharma and Mandal, 2017). There were several parameters considered in the creation of these regressions. In addition to OC and  $NH_3$  emissions from agricultural residue burning in the IGP, emissions of  $NO_x$  and  $N_2O$  were also considered in the creation of the models, however they were determined statistically insignificant by SAS. In addition to emissions from agricultural residue burning in the IGP, several meteorological parameters were considered when creating these equations (e.g. specific humidity, temperature, precipitation, surface layer height, pressure and wind speed). Recall the regression was designed such that SAS picked the variables that created the best fit regression. Furthermore, it is important to note that only days where the air mass originated from biomass burning in the IGP were considered in the creation of the regressions.

The first equation predicts  $PM_{2.5}$  concentrations in April–May, considering both wheat residue emissions from agricultural burning in the IGP as well as meteorological conditions during this time (Equation (2);  $r^2 = 0.40$ ,  $n = 75$ ):

$$PM_{2.5} = 8.31E-7 * E_{OC}^{0.04*} E_{NH_3}^{-0.05*} \exp(-1.5*HLML - 16.36*QLML + 0.40*TLML) \quad (2)$$

where  $E_{NH_3}$  are emissions of  $NH_3$  from agricultural burning in the IGP ( $g \text{ day}^{-1}$ ) for April–May,  $E_{OC}$  are emissions of OC from agricultural burning in the IGP ( $g \text{ day}^{-1}$ ) for April–May, HLML is the daily average surface layer height (m), QLML is the daily average surface specific humidity (1), and TLML is the average daily surface temperature (K).

$PM_{2.5}$  concentrations were also predicted in New Delhi in October–November based on the following equation, which is a function of rice paddy residue emissions and meteorological conditions (Equation (3);  $r^2 = 0.61$ ,  $n = 113$ ):

$$PM_{2.5} = 8.89E6 * E_{NH_3}^{-0.68*} E_{OC}^{0.72*} \exp(-2.56*HLML - 0.17*WS + 0.53*TLML) \quad (3)$$

where  $E_{NH_3}$  are emissions of  $NH_3$  from agricultural burning in the IGP ( $g \text{ day}^{-1}$ ) for October–November,  $E_{OC}$  are emissions of OC from agricultural burning in the IGP ( $g \text{ day}^{-1}$ ) for October–November, HLML is the daily average surface layer height (m), WS is the daily average wind speed at the surface ( $m \text{ s}^{-1}$ ) and TLML is the daily average surface temperature (K). These regressions equations were run for the study period on days where the air mass originated from areas of agricultural burning in the IGP and compared against the ambient  $PM_{2.5}$  measurements using several statistical comparisons to determine how well the models perform. The statistical parameters include the mean normalized bias (MNB), the normalized mean bias (NMB), the normalized mean error (NME) and the normalized mean bias factor (NMBF) (Table 3). These statistical parameters were all included to provide a complete and robust statistical analysis following the work of Tong and Mauzerall (2006) and Zhang et al. (2006).

### 3. Results and discussion

Average daily  $PM_{2.5}$  concentrations in New Delhi were examined for 2016 and 2017 (Fig. 1). Daily average concentrations of  $PM_{2.5}$  ranged from  $22.43 \mu\text{g m}^{-3}$  to  $718.94 \mu\text{g m}^{-3}$ , with an average concentration of  $127.15 \mu\text{g m}^{-3}$  (standard deviation:  $\pm 95.23 \mu\text{g m}^{-3}$ ). According to the Central Pollution Control Board, the Indian Air Quality Standard for  $PM_{2.5}$  (daily average) is  $60 \mu\text{g m}^{-3}$ . In 2016 and 2017, this standard

**Table 3**

Statistical comparisons used in this work. N is the number of observations,  $E_m$  are the emissions projected by the regression model, and  $E_c$  are the emissions calculated in this study.

Parameter	Equation
Mean Normalized Bias	$MNB = \frac{1}{N} \sum_{i=1}^N \left( \frac{E_m(i) - E_c(i)}{E_c(i)} \right)$
Normalized Mean Bias	$NMB = \frac{1}{N} \frac{\sum_{i=1}^N E_m(i) - E_c(i)}{\sum_{i=1}^N E_c(i)}$
Normalized Mean Error	$NME = \frac{1}{N} \frac{\sum_{i=1}^N  E_m(i) - E_c(i) }{\sum_{i=1}^N  E_c(i) }$
Normalized Mean Bias Factor	$NMBF = \left[ \frac{\frac{1}{N} \sum_{i=1}^N E_m}{\frac{1}{N} \sum_{i=1}^N E_c} \right] - 1$ For $\frac{1}{N} \sum_{i=1}^N E_m \geq \frac{1}{N} \sum_{i=1}^N E_c$ $ORNMBF = 1 - \left[ \frac{\frac{1}{N} \sum_{i=1}^N E_c}{\frac{1}{N} \sum_{i=1}^N E_m} \right]$ For $\frac{1}{N} \sum_{i=1}^N E_m < \frac{1}{N} \sum_{i=1}^N E_c$

was exceeded ~75% of the time. Based on Fig. 1, it is evident that concentrations of  $PM_{2.5}$  peak in November, which can likely be attributed to rice paddy residue burning that occurs after the rice paddy harvest as well as meteorological conditions. The meteorological conditions in the IGP during October–November typically include light winds, a low planetary boundary layer and a stable atmosphere, which causes the smoke from these paddy residue burns to blanket much of the IGP and severely deteriorate air quality (Badarinath et al., 2009; Mishra and Shibata, 2012; Singh and Kaskaoutis, 2017).

Emissions of reactive nitrogen species ( $NH_3$ ,  $NO_x$  and  $N_2O$ ) and organic carbon (OC) from agricultural burning were examined for April–May, which is typically the period when wheat residue is burned in the IGP, and October–November, which is typically the period when rice paddy residue is burned in the IGP. For 2016 and 2017, the agricultural burning emissions of  $NH_3$  in the IGP ranged from ~143  $kg \text{ day}^{-1}$  to 908,000  $kg \text{ day}^{-1}$  (standard deviation:  $\pm 161,000 \text{ kg day}^{-1}$ ) in April–May. Emissions of  $NO_x$  from agricultural burning in the IGP in April–May, ranged from ~187  $kg \text{ day}^{-1}$  to  $1.29 \times 10^6 \text{ kg day}^{-1}$  (standard deviation:  $\pm 210,000 \text{ kg day}^{-1}$ ), while emission of  $N_2O$  ranged from ~81  $kg \text{ day}^{-1}$  to 562,000  $kg \text{ day}^{-1}$  (standard deviation:  $\pm 92,000 \text{ kg day}^{-1}$ ). Emissions of OC from agricultural burning in the IGP ranged from ~132  $kg \text{ day}^{-1}$  to 912,000  $kg \text{ day}^{-1}$  (standard deviation:  $\pm 36,000 \text{ kg day}^{-1}$ ) in April and May. In October–November, emissions of  $NH_3$  from agricultural burning ranged from ~3  $kg \text{ day}^{-1}$  to  $2.27 \times 10^7 \text{ kg day}^{-1}$  (standard deviation:  $\pm 2.24 \times 10^6 \text{ kg day}^{-1}$ ), emissions of  $NO_x$  from agricultural burning in the IGP ranged from ~1.5  $kg \text{ day}^{-1}$  to  $1.28 \times 10^7 \text{ kg day}^{-1}$  (standard deviation:  $\pm 1.37 \times 10^6 \text{ kg day}^{-1}$ ), and emissions of  $N_2O$  ranged from ~0.32  $kg \text{ day}^{-1}$  to  $2.68 \times 10^6 \text{ kg day}^{-1}$  (standard deviation:  $\pm 2.87 \times 10^5 \text{ kg day}^{-1}$ ). Emissions of OC from biomass burning in the IGP ranged from ~4  $kg \text{ day}^{-1}$  to  $3.02 \times 10^7 \text{ kg day}^{-1}$  (standard deviation:  $\pm 1.28 \times 10^6 \text{ kg day}^{-1}$ ) during October–November in the study period. Emissions of pollutants from the burning of rice paddy residue tended to be higher than the emissions from the burning of wheat residue, which was expected because much of the wheat residue is used for animal feed (Badarinath et al., 2006).

In order to determine if the spike in the daily average  $PM_{2.5}$  concentration can be partially attributed to agricultural burning in the IGP, back trajectory analysis was performed using the NOAA HYSPLIT model (<https://ready.arl.noaa.gov/HYSPLIT.php>). Two events were analyzed using the HYSPLIT model. The first analysis is on November 6, 2016. During this time, the daily average  $PM_{2.5}$  concentration in New

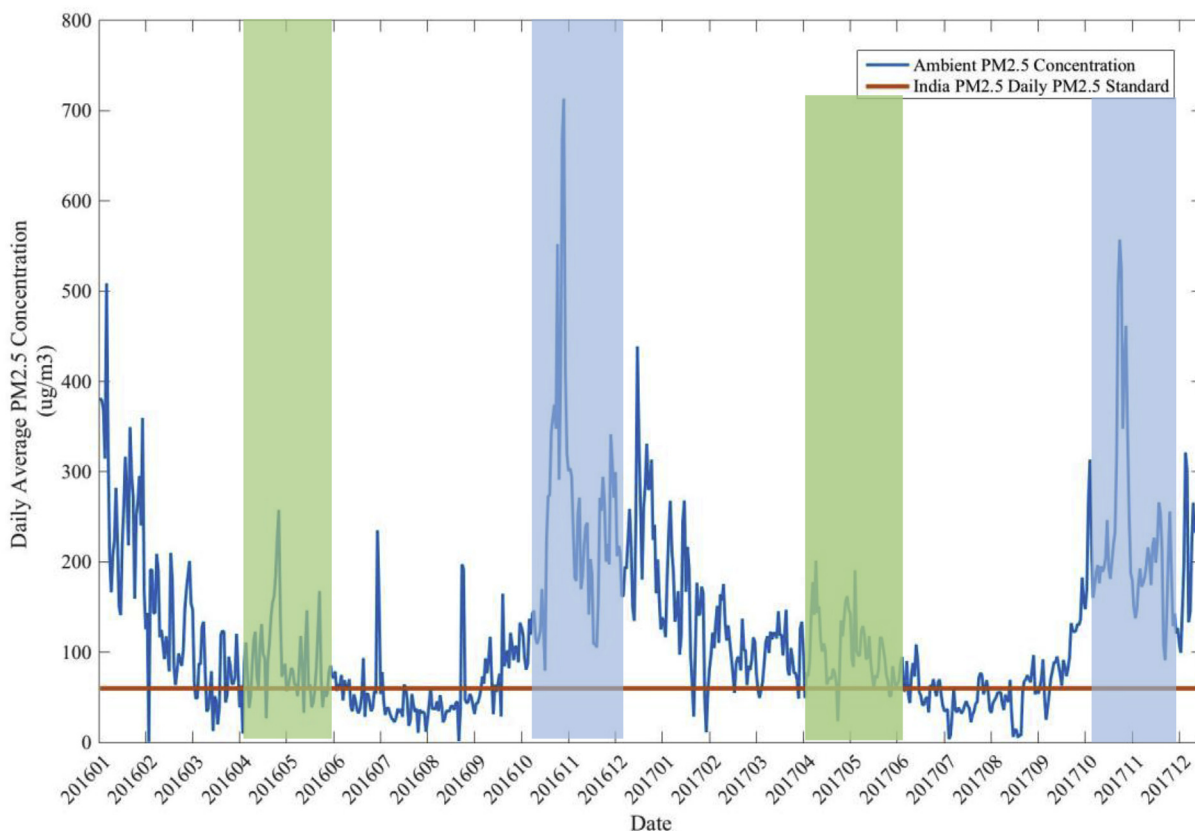


**Fig. 1.** Daily average concentrations of PM<sub>2.5</sub> concentrations in New Delhi, India. The blue line represents the average daily concentrations of PM<sub>2.5</sub>, while the red line represents the Indian Ambient Air Quality Standards for PM<sub>2.5</sub>. The green shading represents periods of wheat residue burning while the blue shading represents periods of rice paddy residue burning. (For interpretation of the references to colour in this figure legend, the reader is referred to the Web version of this article.)

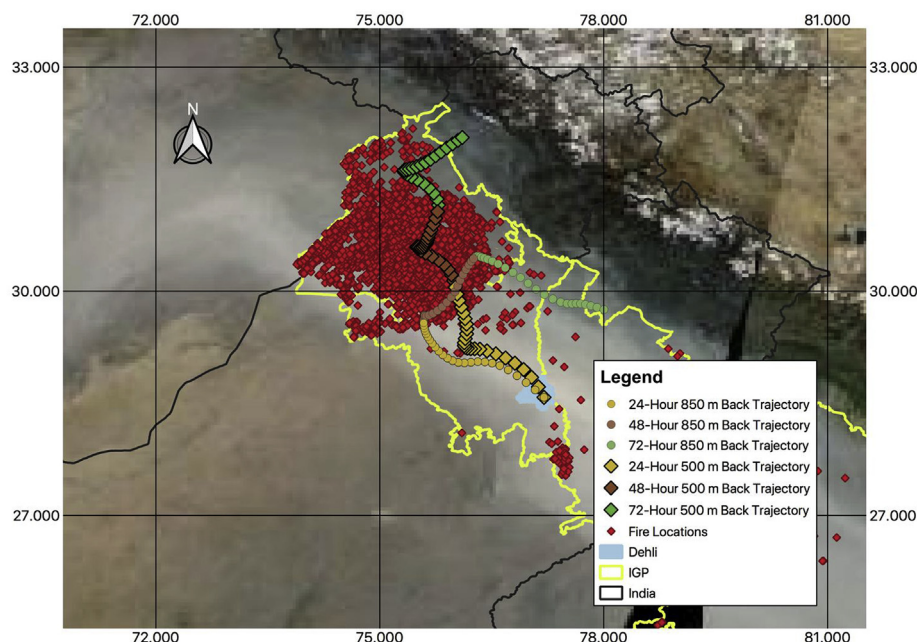


**Fig. 2.** NASA FIRMS active fire data (MODIS MCD14DL) plotted the 24-h back trajectory (500 m) for November 6, 2016, from the NOAA HYSPLIT model. The background image is a MODIS image from NASA's Terra satellite for November 6, 2016, that shows smoke blanketing the region. The units of the latitude and longitude are degrees.

Delhi, India, peaked at  $718.94 \mu\text{g m}^{-3}$  (standard deviation:  $\pm 204.24 \mu\text{g m}^{-3}$ ), which is a factor of  $\sim 12$  higher than the standard for daily average PM<sub>2.5</sub> concentration. When running the HYSPLIT model for 24-h, 48-h and 72-h back trajectories at both 500 m and 850 m for 11 a.m. for this time frame, it is evident that agricultural burning emissions are being transported to New Delhi from the IGP

(Fig. 2). These time periods and heights were chosen in order to get a good representation of where the air mass originated. It is evident from the MODIS (Terra) snapshot (Fig. 2, background), smoke from the agricultural burns on during the first week of November 2016, is blanketing much of the IGP.

The second back trajectory analysis focuses on May 29th, 2016

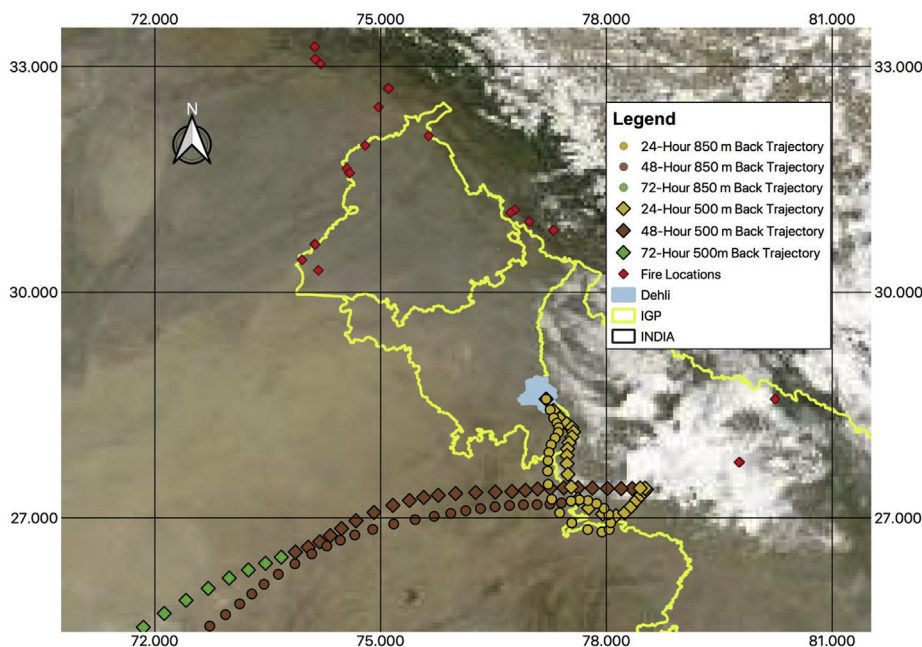


Fig. 3. NASA FIRMS active fire data (MODIS MCD14DL) plotted the 24-h back trajectory (500 m) for May 29, 2016, from the NOAA HYSPLIT model. The background image is a MODIS image from NASA's Terra satellite for May 29, 2016. The units of the latitude and longitude are degrees.

(Fig. 3). During this time, the average daily concentration of  $PM_{2.5}$  was  $38.89 \mu g m^{-3}$  (standard deviation:  $\pm 34.48 \mu g m^{-3}$ ), which is a factor of 0.65 lower than the national ambient air quality standard. In contrast to the previous analysis, the back trajectory for this period shows that the air mass came from the south, where no burning was occurring, instead of from the IGP (Fig. 3). When looking at the MODIS imagery for May 29, 2016, it is evident that while there is some burning over the IGP, the smoke emissions are not having a major impact on New Delhi, India.

In addition to this, the average ambient concentrations of  $PM_{2.5}$  in New Delhi when agricultural burning emissions were impacting the area were compared against the average ambient concentrations when biomass burning emissions were not impacting the area (Fig. 4). When agricultural residue burning emissions were not influencing New Delhi, the average ambient  $PM_{2.5}$  concentration in April/May was

$75.6 \mu g m^{-3}$  (standard deviation:  $\pm 23.3 \mu g m^{-3}$ ) while the average ambient concentration in October/November was  $122.1 \mu g m^{-3}$  (standard deviation:  $\pm 11.9 \mu g m^{-3}$ ). In contrast to this, the average ambient concentrations of  $PM_{2.5}$  in New Delhi under the influence of agricultural residue burning emissions were  $111.1 \mu g m^{-3}$  (standard deviation:  $\pm 40.1 \mu g m^{-3}$ ) in April/May and  $215.4 \mu g m^{-3}$  (standard deviation:  $\pm 125.4 \mu g m^{-3}$ ) in October/November. This suggests that emissions from agricultural residue burning in the IGP likely contributes to an ~35% increase in ambient  $PM_{2.5}$  concentrations in New Delhi, India.

Statistical regression models were created to be able to predict the daily average  $PM_{2.5}$  concentration in New Delhi, India, based on emissions of  $NH_3$  from wheat residue burning and rice paddy residue burning in the IGP and meteorological conditions. These regressions were then run against the data used in this study (Fig. 5). The average

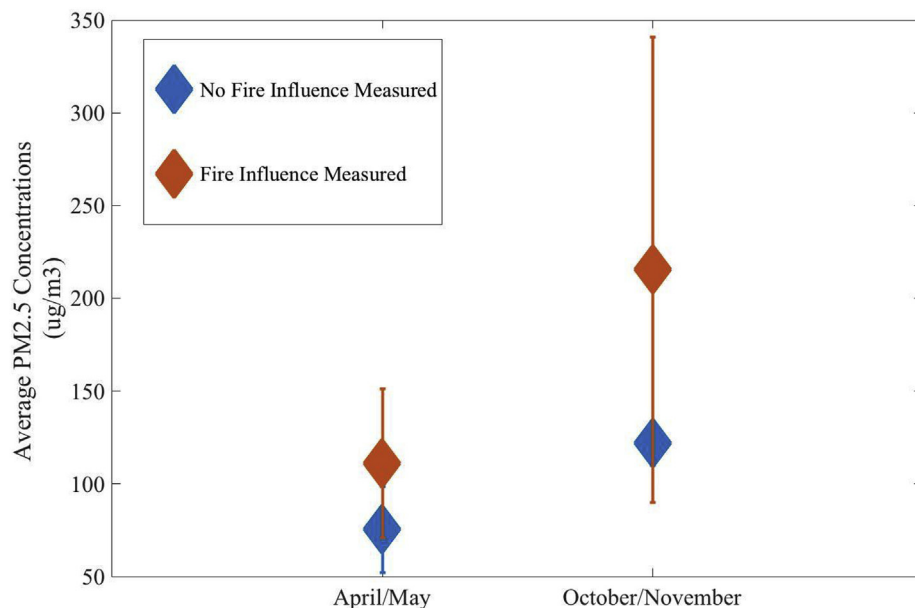
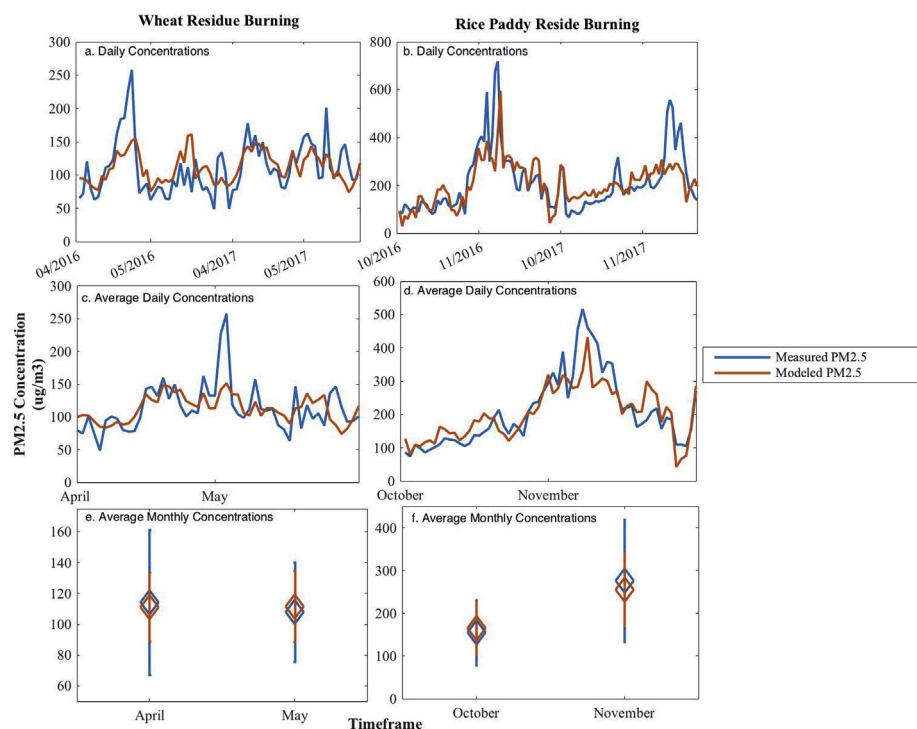


Fig. 4. Comparison of measured ambient  $PM_{2.5}$  concentrations in New Delhi, India, from agricultural residue burning emissions in the IGP for April/May and October/November during periods when emissions were impacting and not impacting the air quality in New Delhi, India. The error bands represent one standard deviation.



**Fig. 5.** Comparing measured ambient  $PM_{2.5}$  concentrations in New Delhi, India, with  $PM_{2.5}$  concentrations modeled by both regressions. Fig. 5a shows both modeled (red line) and measured (blue line) concentrations of  $PM_{2.5}$  for each day during the study period for wheat residue burning while Fig. 5b shows both the modeled (red line) and measured (blue line) concentrations of  $PM_{2.5}$  in New Delhi during the study period of rice paddy residue burning. Fig. 5c and d both show the average daily modeled (red line) and measured (blue line) concentrations of  $PM_{2.5}$  for April/May and October/November, respectively. Fig. 5e and f both show the average monthly concentration of  $PM_{2.5}$  measured (blue line) and modeled (red line) for the study period for April/May and October/November, respectively. (For interpretation of the references to colour in this figure legend, the reader is referred to the Web version of this article.)

**Table 4**

Comparison statistics for daily average  $PM_{2.5}$  concentration in New Delhi, India, during April–May and October–November 2016 and 2017.

	$PM_{2.5}$ Concentrations (April–May) ( $\mu\text{g m}^{-3}$ )	$PM_{2.5}$ Concentrations (October–November) ( $\mu\text{g m}^{-3}$ )
<b>Observations</b>		
Average	111.2	211.5
Standard Deviation	40.4	127.0
Max	257.7	719.0
Median	103.3	178.1
<b>Model</b>		
Average	111.4	207.1
Standard Deviation	22.5	86.6
Max	160.8	595.0
Median	109.5	199.8
<b>Comparison Statistics</b>		
Mean Normalized Bias (%)	8.27	8.73
Normalized Mean Bias (%)	0.003	−0.02
Normalized Mean Error (%)	0.30	0.25
Normalized Mean Bias Factor (%)	0.21	−2.13
Ratio of average measured value to average modeled value	0.94	0.89
Ratio of median measured value to median modeled value	0.99	1.02
Correlation Coefficient ( $r$ )	0.35	0.51
Number of Observations	76	116

$PM_{2.5}$  emissions predicted by the models were, on average,  $111.4 \mu\text{g m}^{-3}$  (standard deviation:  $\pm 22.5 \mu\text{g m}^{-3}$ ) for April/May (compared against observed concentrations of  $111.2 \pm 40.4 \mu\text{g m}^{-3}$ ) while concentrations predicted by the October/November regressions were, on average,  $207 \pm 87 \mu\text{g m}^{-3}$  (compared against observed concentrations of  $PM_{2.5}$  in New Delhi of  $212 \pm 127 \mu\text{g m}^{-3}$ ). When comparing the regression model with the observed concentrations for April–May, the mean normalized bias was 8.27%, the normalized mean bias was 0.003%, the normalized mean error was 0.30% and the normalized mean bias factor was 0.21%. When comparing the regression model for October–November against the observed values (Table 4), the mean normalized bias was 8.73%, the normalized mean bias was  $-0.02\%$ , the normalized mean error was 0.25% and the normalized mean bias factor was  $-2.13\%$ . Both models predict the  $PM_{2.5}$  observations well. An important benefit of these regression models is that they are a computationally inexpensive way to be able to predict

concentrations of  $PM_{2.5}$  during times of agricultural residue burning.

#### 4. Conclusions

Fine particulate matter measured concentrations in New Delhi, India, were on average  $127.15 \mu\text{g m}^{-3} \pm 95.23 \mu\text{g m}^{-3}$ . Through the two-year period (2016–2017), concentrations of  $PM_{2.5}$  in New Delhi exceeded the national standard of  $60 \mu\text{g m}^{-3}$  approximately 75% of the time. As expected, the highest concentrations of  $PM_{2.5}$  occurred when agricultural burning of rice paddy residue was occurring in the IGP. Emissions of reactive nitrogen species from wheat residue burning were lower than emissions from rice paddy residue burning, which is attributed to more favorable meteorological conditions for smoke dispersal as well as less mass burned. Two days in the study period were examined to determine the origin of the air mass arriving in New Delhi, India. The first analysis is on November 6, 2016, during which time the

daily average measured concentration of PM<sub>2.5</sub> in New Delhi was  $718.94 \mu\text{g m}^{-3} \pm 204.24 \mu\text{g m}^{-3}$ , which is a factor of 11.98 higher than the standard for daily average PM<sub>2.5</sub> concentration. The 24-h back trajectory for this day shows that the air mass came directly from a region of the IGP that experienced vast agricultural burning, which was blanketing much of the IGP with smoke. The second day (May 29, 2016) chosen for analysis was a day when the average concentration of PM<sub>2.5</sub> was much lower ( $38.89 \mu\text{g m}^{-3} \pm 34.48 \mu\text{g m}^{-3}$ , which is a factor of 0.65 lower than the national standard). For this analysis, the 24-h back trajectory showed that the air mass came from the south/southeast and there were few agricultural burns impacting the IGP. Agricultural residue burning emits significant amounts of reactive nitrogen species, including NH<sub>3</sub>, which is an important precursor gas for the formation of secondary fine particulate matter, into the atmosphere. Therefore, two statistical regression models were developed to predict average daily PM<sub>2.5</sub> concentrations in New Delhi, India, based on emissions of NH<sub>3</sub> and OC in the IGP from wheat residue burning/rice paddy residue burning and meteorological conditions. The average modeled concentration of PM<sub>2.5</sub> in New Delhi, India, were  $98 \mu\text{g m}^{-3}$  (standard deviation:  $\pm 34 \mu\text{g m}^{-3}$ ) during April/May and  $210 \mu\text{g m}^{-3} \pm 86 \mu\text{g m}^{-3}$  during October/November. When comparing the regression results with the observational data, both models were similar to the average observations.

#### Declaration of competing interest

The authors declare that they have no known competing financial interests or personal relationships that could have appeared to influence the work reported in this paper.

#### Acknowledgements

We thank Dr. Nalin Agarwal, Climate Collective, and Dr. Prashant Gargava, Central Pollution Control Board, both in New Delhi, India, for their assistance in providing the data. We acknowledge the NASA Land Processes Distributed Active Archive Center (LP DAAC) for freely providing the MODIS VCF data and the University of Maryland for generously providing the MODIS burn area data, which are freely available from <http://modis-fire.umd.edu/ba.html>. The authors would also like to acknowledge and thank NASA for providing the MERRA-2 data on their website (<https://gmao.gsfc.nasa.gov/reanalysis/MERRA-2/>). We would like to acknowledge the NOAA Air Resources Laboratory for providing their HYSPLIT model online (<https://ready.arl.noaa.gov/HYSPLIT.php>) and OpenAQ ([openaq.org](https://openaq.org)) for freely providing ambient measurements of PM<sub>2.5</sub> in India.

#### References

- Andreae, M.O., Merlet, P., 2001. Emission of trace gases and aerosols from biomass burning. *Glob. Biogeochem. Cycles* 15, 955–966.
- Arola, A., Lindfors, A., Natunen, A., Lehtinen, K., 2007. A case study on biomass burning aerosols: effects on aerosol optical properties and surface radiation levels. *Atmos. Chem. Phys.* 7, 4257–4266.
- Badarinath, K., Kharol, S.K., Sharma, A.R., Prasad, V.K., 2009. Analysis of aerosol and carbon monoxide characteristics over arabian sea during crop residue burning period in the indo-gangetic plains using multi-satellite remote sensing datasets. *J. Atmos. Sol. Terr. Phys.* 71, 1267–1276.
- Badarinath, K., Chand, T., Prasad, V.K., 2006. Agriculture crop residue burning in the indo-gangetic plains—A study using IRS-P6 AWiFS satellite data. *Curr. Sci.* 91, 00113891.
- Baek, B.H., Aneja, V.P., Tong, Q., 2004. Chemical coupling between ammonia, acid gases, and fine particles. *Environ. Pollut.* 129, 89–98. Available at: <https://www.meas.ncsu.edu/airquality/pubs/pdfs/Ref%20103.pdf>.
- Baek, B.H., Aneja, V.P., 2004. Measurement and analysis of the relationship between ammonia, acid gases, and fine particles in Eastern North Carolina. *J. Air Waste Manag. Assoc.* 54, 623–633. Available at: <https://www.meas.ncsu.edu/airquality/pubs/pdfs/Ref%20104.pdf>.
- Battye, W., Aneja, V.P., Schlesinger, W.H., 2017. Is nitrogen the next carbon? *Earth's Future* 5, 894–904. <https://doi.org/10.1002/2017EF000592>.
- Behera, S.N., Sharma, M., 2010. Investigating the potential role of ammonia in ion chemistry of fine particulate matter formation for an urban environment. *Sci. Total Environ.* 408, 3569–3575.
- Bisht, D., Dumka, U., Kaskaoutis, D., Piplal, A., Srivastava, A., Soni, V., Attri, S., Sateesh, M., Tiwari, S., 2015. Carbonaceous aerosols and pollutants over Delhi urban environment: temporal evolution, source apportionment and radiative forcing. *Sci. Total Environ.* 521, 431–445.
- Christian, T.J., Kleiss, B., Yokelson, R.J., Holzinger, R., Crutzen, P.J., Hao, W.M., Saharjo, B.H., Ward, D.E., 2003. Comprehensive laboratory measurements of biomass-burning emissions: 1. Emissions from Indonesian, African, and other fuels. *J. Geophys. Res.: Atmosphere* 108 (D23).
- Crouse, D.L., Peters, P.A., van Donkelaar, A., Goldberg, M.S., Villeneuve, P.J., Brion, O., Khan, S., Atari, D.O., Jerrett, M., Pope III, C.A., 2015. Risk of nonaccidental and cardiovascular mortality in relation to long-term exposure to low concentrations of fine particulate matter: a Canadian national-level cohort study. *Environ. Health Perspect.* 120 (5), 708–714.
- Dimiceli, C., Carroll, M., Sohlberg, R., Kim, D.H., Kelly, M., Townshend, J.R.G., 2015. MOD44B MODIS/Terra vegetation continuous fields yearly L3 global 250m SIN grid V006 [data set]. NASA EOSDIS Land Processes DAAC. <https://doi.org/10.5067/MODIS/MOD44B.006>.
- DiMiceli, C.M., Carroll, M., Sohlberg, R., Huang, C., Hansen, M.C., Townshend, J.R.G., 2017. Annual Global Automated MODIS Vegetation Continuous Fields (MOD44B) at 250 M Spatial Resolution for Data Years Beginning Day 65, 2000–2014, Collection 5 Percent Tree Cover. University of Maryland, College Park, MD, USA version 6.
- Eurachem/CITAC Working Group, Eurachem and Co-operation on International Traceability in Analytical Chemistry, 2000. Quantifying Uncertainty in Analytical Measurement. Eurachem.
- Fan, J., Zhang, R., Li, G., Nielsen-Gammon, J., Li, Z., 2005. Simulations of fine particulate matter (PM<sub>2.5</sub>) in Houston, Texas. *J. Geophys. Res.: Atmosphere* 110.
- Freitas, S.R., Longo, K.M., Dias, M.A.S., Dias, P.L.S., Chatfield, R., Prins, E., Artaxo, P., Grell, G.A., Recuero, F.S., 2005. Monitoring the transport of biomass burning emissions in south America. *Environ. Fluid Mech.* 5, 135–167.
- Gelaro, R., McCarty, W., Suárez, M.J., Todling, R., Molod, A., Takacs, L., Randles, C.A., Darmenov, A., Bosilovich, M.G., Reichle, R., 2017. The modern-era retrospective analysis for research and applications, version 2 (MERRA-2). *J. Clim.* 30, 5419–5454.
- Giglio, L., Boschetti, L., Roy, D.P., Humber, M.L., Justice, C.O., 2018. The collection 6 MODIS burned area mapping algorithm and product. *Remote Sens. Environ.* 217, 72–85.
- Giglio, L., Desloitures, J., Justice, C.O., Kaufman, Y.J., 2003. An enhanced contextual fire detection algorithm for MODIS. *Remote Sens. Environ.* 87, 273–282.
- Giglio, L., Justice, C., Boschetti, L., Roy, D., 2015. MCD64A1 MODIS/Terra+ Aqua burned area monthly L3 global 500m SIN grid V006 [data set]. NASA EOSDIS Land Processes DAAC. <https://doi.org/10.5067/MODIS/MCD64A1.006>.
- Global Modeling, Assimilation Office (GMAO), 2015. MERRA-2 inst1\_2d\_lfo.Nx: 2d,1-Hourly,Instantaneous,Single-Level,Assimilation,Land surface forcings V5.12.4, greenbelt, MD, USA, goddard earth sciences data and information services center (GES DISC). Accessed: January 2019, 10.5067/RCMZA6TL70BG.
- Gupta, P.K., Sahai, S., Singh, N., Dixit, C., Singh, D., Sharma, C., Tiwari, M., Gupta, R.K., Garg, S., 2004. Residue burning in rice-wheat cropping system: causes and implications. *Curr. Sci.* 1713–1717.
- Hays, M.D., Fine, P.M., Geron, C.D., Kleeman, M.J., Gullett, B.K., 2005. Open burning of agricultural biomass: Physical and chemical properties of particle-phase emissions. *Atmospheric Environment* 39 (36), 6747–6764.
- Heald, C.L., JI Jr., C., Lee, T., Benedict, K., Schwandner, F., Li, Y., Clarisse, L., Hurtmans, D., Van Damme, M., Clerbaux, C., 2012. Atmospheric Ammonia and Particulate Inorganic Nitrogen over the United States.
- Ito, A., Penner, J.E., 2004. Global estimates of biomass burning emissions based on satellite imagery for the year 2000. *J. Geophys. Res.: Atmosphere* 109.
- Kanabkaew, T., Oanh, N.T.K., 2011. Development of spatial and temporal emission inventory for crop residue field burning. *Environ. Model. Assess.* 16, 453–464.
- Kanokkanjana, K., Cheewaphongphan, P., Garivait, S., 2011. Black carbon emission from paddy field open burning in Thailand. *IPCBE Proc* 6, 88–92.
- Kaskaoutis, D., Kumar, S., Sharma, D., Singh, R.P., Kharol, S., Sharma, M., Singh, A., Singh, S., Singh, A., Singh, D., 2014. Effects of crop residue burning on aerosol properties, plume characteristics, and long-range transport over northern India. *J. Geophys. Res.: Atmosphere* 119, 5424–5444.
- Kharol, S.K., Badarinath, K., Sharma, A.R., Mahalakshmi, D., Singh, D., Prasad, V.K., 2012. Black carbon aerosol variations over Patiala city, Punjab, India—a study during agriculture crop residue burning period using ground measurements and satellite data. *J. Atmos. Sol. Terr. Phys.* 84, 45–51.
- Mishra, A.K., Shibata, T., 2012. Synergistic analyses of optical and microphysical properties of agricultural crop residue burning aerosols over the indo-gangetic basin (IGB). *Atmos. Environ.* 57, 205–218.
- NASA Near Real-Time and MCD14DL MODIS Active Fire Detections (SHP format). Data set. Available on-line [<https://earthdata.nasa.gov/active-fire-data>].
- Ni, H., Tian, J., Wang, X., Wang, Q., Han, Y., Cao, J., Long, X., Chen, L.W.A., Chow, J.C., Watson, J.G., Huang, R.J., 2017. PM<sub>2.5</sub> emissions and source profiles from open burning of crop residues. *Atmos. Environ.* 169, 229–237.
- Pant, P., Shukla, A., Kohl, S.D., Chow, J.C., Watson, J.G., Harrison, R.M., 2015. Characterization of ambient PM<sub>2.5</sub> at a pollution hotspot in New Delhi, India and inference of sources. *Atmos. Environ.* 109, 178–189.
- Paulot, F., Jacob, D.J., 2014. Hidden cost of U.S. Agricultural exports: particulate matter from ammonia emissions. *Environ. Sci. Technol.* 48, 903–908. <https://doi.org/10.1021/es4034793>.
- Pittman, K., Hansen, M.C., Becker-Reshef, I., Potapov, P.V., Justice, C.O., 2010. Estimating global cropland extent with multi-year MODIS data. *Remote Sens.* 2, 1844–1863.
- Pope III, C.A., Ezzati, M., Dockery, D.W., 2009. Fine-particulate air pollution and life

- expectancy in the United States. *N. Engl. J. Med.* 360, 376–386.
- Pope III, C.A., Dockery, D.W., 2006. Health effects of fine particulate air pollution: lines that connect. *J. Air Waste Manag. Assoc.* 56, 709–742.
- Pope III, C.A., Burnett, R.T., Thun, M.J., Calle, E.E., Krewski, D., Ito, K., Thurston, G.D., 2002. Lung cancer, cardiopulmonary mortality, and long-term exposure to fine particulate air pollution. *Jama* 287, 1132–1141.
- Ravindra, K., Singh, T., Mor, S., 2019. Emissions of air pollutants from primary crop residue burning in India and their mitigation strategies for cleaner emissions. *J. Clean. Prod.* 208, 261–273.
- Rajput, P., Sarin, M.M., Sharma, D., Singh, D., 2014. Atmospheric polycyclic aromatic hydrocarbons and isomer ratios as tracers of biomass burning emissions in Northern India. *Environ. Sci. Pollut. Control Ser.* 21 (8), 5724–5729.
- Rajput, P., Sarin, M., Sharma, D., Singh, D., 2016. Characteristics and emission budget of carbonaceous species from post-harvest agricultural-waste burning in source region of the Indo-Gangetic Plain. In: *Air Quality*. Apple Academic Press, pp. 271–292.
- Rienecker, M.M., Suarez, M.J., Gelaro, R., Todling, R., Bacmeister, J., Liu, E., Bosilovich, M.G., Schubert, S.D., Takacs, L., Kim, G., 2011. MERRA: NASA's modern-era retrospective analysis for research and applications. *J. Clim.* 24, 3624–3648.
- Roy, D.P., Boschetti, L., Justice, C.O., Ju, J., 2008. The collection 5 MODIS burned area product—global evaluation by comparison with the MODIS active fire product. *Remote Sens. Environ.* 112, 3690–3707.
- Roy, D., Jin, Y., Lewis, P., Justice, C., 2005. Prototyping a global algorithm for systematic fire-affected area mapping using MODIS time series data. *Remote Sens. Environ.* 97, 137–162.
- Roy, D., Lewis, P., Justice, C., 2002. Burned area mapping using multi-temporal moderate spatial resolution data—a bi-directional reflectance model-based expectation approach. *Remote Sens. Environ.* 83, 263–286.
- Sahai, S., Sharma, C., Singh, S., Gupta, P.K., 2011. Assessment of trace gases, carbon and nitrogen emissions from field burning of agricultural residues in India. *Nutrient Cycl. Agroecosyst.* 89, 143–157.
- Scholes, R., Ward, D., Justice, C., 1996. Emissions of trace gases and aerosol particles due to vegetation burning in southern hemisphere africa. *J. Geophys. Res.: Atmosphere* 101, 23677–23682.
- Schwartz, J., Laden, F., Zanobetti, A., 2002. The concentration-response relation between PM<sub>2.5</sub> and daily deaths. *Environ. Health Perspect.* 110, 1025–1029.
- Seiler, W., Crutzen, P.J., 1980. Estimates of gross and net fluxes of carbon between the biosphere and the atmosphere from biomass burning. *Clim. Change* 2, 207–247.
- Sharma, D., Singh, M., Singh, D., 2011. Impact of post-harvest biomass burning on aerosol characteristics and radiative forcing over patiala, north-west region of India. *J. Inst. Eng.* 8, 11–24.
- Sharma, S.K., Mandal, T.K., 2017. Chemical composition of fine mode particulate matter (PM<sub>2.5</sub>) in an urban area of Delhi, India and its source apportionment. *Urban Clim.* 21, 106–122.
- Shyamsundar, P., Springer, N.P., Tallis, H., Polasky, S., Jat, M.L., Sidhu, H.S., Krishnapriya, P.P., Skiba, N., Ginn, W., Ahuja, V., Cummins, J., Datta, I., Dholakia, H.H., Dixon, J., Gerard, B., Gupta, R., Hellmann, J., Jadhav, A., Jat, H.S., Keil, A., Ladha, J.K., Lopez-Ridauro, S., Nandrajog, S.P., Paul, S., Ritter, A., Sharma, P.C., Singh, R., Singh, D., Somanathan, R., 2019. Fields on fire: Alternatives to crop residue burning in India. *Science* 365 (6453), 536–538.
- Singh, R.P., Kaskaoutis, D.G., 2017. Crop residue burning: a threat to South Asian air quality. *Eos, Transactions American Geophysical Union* 333–334 95.
- Tong, D.Q., Mauzerall, D.L., 2006. Spatial variability of summertime tropospheric ozone over the continental United States: implications of an evaluation of the CMAQ model. *Atmos. Environ.* 40 (17), 3041–3056.
- Vadrevu, K.P., Ellicott, E., Badarinath, K., Vermote, E., 2011. MODIS derived fire characteristics and aerosol optical depth variations during the agricultural residue burning season, north India. *Environ. Pollut.* 159, 1560–1569.
- Wang, X., Wang, W., Yang, L., Gao, X., Nie, W., Yu, Y., Xu, P., Zhou, Y., Wang, Z., 2012. The secondary formation of inorganic aerosols in the droplet mode through heterogeneous aqueous reactions under haze conditions. *Atmos. Environ.* 63, 68–76.
- Wiedinmyer, C., Akagi, S., Yokelson, R.J., Emmons, L., Al-Saadi, J., Orlando, J., Soja, A., 2011. The fire INventory from NCAR (FINN): a high resolution global model to estimate the emissions from open burning. *Geosci. Model Dev. (GMD)* 4, 625.
- Wiedinmyer, C., Quayle, B., Geron, C., Belote, A., McKenzie, D., Zhang, X., O'Neill, S., Wynne, K.K., 2006. Estimating emissions from fires in North America for air quality modeling. *Atmos. Environ.* 40, 3419–3432.
- Yang, S., He, H., Lu, S., Chen, D., Zhu, J., 2008. Quantification of Crop Residue Burning in the Field and its Influence on Ambient Air Quality in Suqian, China. *Atmospheric Environment* 42, 1961–1969.
- Zhang, Y., Liu, P., Pun, B., Seigneur, C., 2006. A comprehensive performance evaluation of MM5-CMAQ for the Summer 1999 Southern Oxidants Study episode—Part I: evaluation protocols, databases, and meteorological predictions. *Atmos. Environ.* 40 (26), 4825–4838.